NONINVASIVE EXTRACTION OF INPUT FUNCTION FROM CAROTID ARTERY IN $H_2{}^{15}O$ DYNAMIC BRAIN POSITRON EMISSION TOMOGRAPHY USING INDEPENDENT COMPONENT ANALYSIS

Ji Young Ahn, Jae Sung Lee, Myoung Jin Jang, and Dong Soo Lee

Department of Nuclear Medicine, Seoul National University College of Medicine,
28 Yungun-Dong, Chongno-Gu, Seoul 110-744, Korea

ABSTRACT

For the absolute quantification of regional cerebral blood flow (rCBF) by means of $H_2{}^{15}O$ positron emission tomography (PET) and kinetic modeling, arterial input function should be determined accurately. Even if arterial blood sampling, as an input function, provides an accurate time-activity curve (TAC), it is invasive and delay from carotid artery to radial artery should be corrected. Since the TAC from the region of interest (ROI) drawn on the small area containing carotid artery could not be determined objectively, more reproducible and objective method for noninvasive derivation of the input function is required. We applied independent component analysis (ICA) to dynamic brain $H_2{}^{15}O$ PET image (canine study) to obtain input function from carotid artery noninvasively. The independent components were estimated by recursively minimizing the mutual information (measure of dependency) among the estimated independent components. We calculated area under the curve (AUC) of input functions from ICA method and from blood samples and compared each other to validate the accuracy of ICA method. ICA successfully extracted carotid artery TACs from the $H_2{}^{15}O$ PET images and their corresponding images. The extracted TACs by ICA method were well correlated with the arterial blood samples.

1. INTORDUCTION

Dynamic brain $H_2{}^{15}O$ positron emission tomography (PET) has been widely used to estimate quantitative regional cerebral blood flow (rCBF). Accurate input function is necessary for the measurement of rCBF. Input function is the time feature of injected radioisotope in arterial blood and the typical shape of input function is shown in Figure 1. There are two ways to obtain input function: invasive blood sampling from artery and noninvasive extraction of input function by drawing the region of interest (ROI) on PET image. Arterial sampling provides accurate input function, however, it is inconvenient and may be harmful to patients. Although the use of ROI is a comfortable method, it may cause to inaccurate input function due to the difficulty in drawing ROI in small carotid artery region.

Factor analysis has been proposed to extract the left ventricular (LV) input function and tissue time-activity curve (TAC) from the $H_2{}^{15}O$ PET image instead of usual ROI method without $C^{15}O$ PET scanning [1]. Recently factor analysis was also applied to extract input function from carotid artery with brain F-18 FDG and $H_2{}^{15}O$ PET [2]. Although the factor analysis is considered as an attractive tool to process dynamic image sequences, the problem of non-uniqueness of the solution makes the user of this method cumbersome [3], [4].

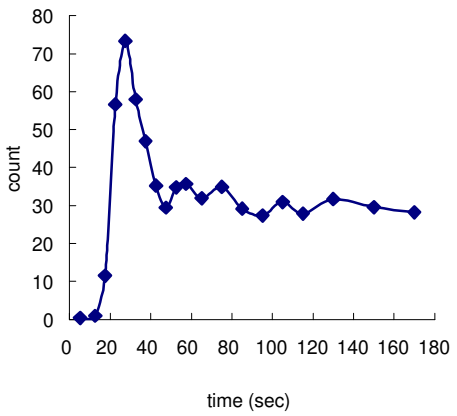

Figure 1. Input function from carotid artery using conventional ROI method from $H_2{}^{15}O$ brain PET image

When radioisotope is injected by bolus, the shape of input function has the characteristic of sparseness.

Independent component analysis (ICA) has been applied to the medical field because of its plausibility to biomedical signals [5], [6], [7], and the applications were mainly about fMRI and EEG data analysis. There was an approach to extract LV input function from $H_2{}^{15}O$ dynamic myocardial PET image using ICA [8] and the result of the approach showed the possibility of ICA application to PET data analysis.

For the application of ICA to PET image, 5 normal dogs were performed dynamic brain $H_2{}^{15}O$ PET scan. Extended ICA was used to extract input function from internal carotid artery without the aid of any other images.

2. INDEPENDENT COMPONENT ANALYSIS

The data obtained by $H_2{}^{15}O$ dynamic brain PET scan is the mixed signal $\boldsymbol{x}(p)$ at each sampling point p. If we assume the linear mixing situation, the relationship between the independent source and its mixture can be written as

$$\boldsymbol{x}(p) = \mathbf{A} \cdot \boldsymbol{s}(p) \tag{1}$$

where $\mathbf{A}$ is a mixing matrix and $\boldsymbol{s}(p)$ is the vector of source signals.

$\boldsymbol{x}(p)$ is composed of pixels (x_1, x_2,¡ ¡¿ ,x_N) and it can be written as $x(p) = [x_1(p), x_2(p), \cdots, x_N(p)]$. Each pixel of each sampling point (frame), x_i, can be described as a mixture of the independent elementary activities as following equations.

$$\begin{aligned} x_1 &= A_{CA,1} \times S_{CA} + A_{V,1} \times S_V + A_{TI,1} \times S_{TI} \\ x_2 &= A_{CA,2} \times S_{CA} + A_{V,2} \times S_V + A_{TI,2} \times S_{TI} \\ &\vdots \\ x_N &= A_{CA,N} \times S_{CA} + A_{V,N} \times S_V + A_{TI,N} \times S_{TI} \end{aligned} \tag{2}$$

where, the random variables S_{CA}, S_V and S_{TI} represent the elementary activities corresponding to the carotid artery, vein and tissue, respectively. Since their anatomical structures are not overlapped in the 3-dimensional space, they can be regarded as independent sources. Thus mixing matrix or basis function, A, represents the contribution of the activity of each anatomical structure to the PET image of each frame. So the vector $[A_{CA,1}\ A_{V,2}\ A_{TI,N}]$ corresponds to the TAC of each structure and S is the matrix of independent component map.

The sources are exactly recovered when $\mathbf{W} = \mathbf{A}^{-1}$. Many methods for ICA have been proposed to find a linear transformation matrix $\mathbf{W}$ and we used extended ICA in this paper.

Extended infomax learning algorithm proposed in [11] to maximize the joint entropy provides a simple learning rule for sources with a variety of distributions. Extended infomax learning rule can be summarized as following equation

$$\Delta \mathbf{W} \propto \left[\mathbf{I} - \mathbf{K} \cdot \tanh(\mathbf{u}) \cdot \mathbf{u}^{\mathrm{T}} - \mathbf{u} \cdot \mathbf{u}^{\mathrm{T}}\right]\mathbf{W} \tag{3}$$

where $\mathbf{K}$ is an N-dimensional diagonal matrix of which diagonal element k_i must be

$$k_i = \operatorname{sign}\left(E\{\operatorname{sech}^2(u_i)\}E\{u_i^2\} - E\{[\tanh(u_i)]u_i\}\right) \tag{4}$$

Log-likelihood of the PDF of the observation described as following equation is a measurement of the independency between the estimates.

$$L(\mathbf{u}, \mathbf{W}) = \log\left|\det(\mathbf{W})\right| + \sum_{i=1}^{N} \log p_i(u_i) \tag{5}$$

3. $H_2{}^{15}O$ PET IMAGE ACQUISITION AND DATA PROCESSING

3.1 Image Acquisition and Reconstruction

$H_2{}^{15}O$ PET scans were performed on five normal dogs at rest and diamox challenge using an ECAT EXACT 47 scanner (Siemens-CTI, Knoxville, USA), which has an intrinsic resolution of 5.2 mm FWHM (full width at half maximum) and images 47 contiguous planes with thickness of 3.4 mm simultaneously for a longitudinal field of view of 16.2 cm. For attenuation correction, transmission scan was performed using three Ge-68 rod sources before $H_2{}^{15}O$ emission scan. For the dynamic emission scan, twelve 5 second, nine 10 second, and three 30 second frames were acquired simultaneously with the bolus injection (injection time < 10 seconds) of 555~740 MBq $H_2{}^{15}O$. Arterial blood sampling was also performed in femoral or radial artery with the same protocol of PET scan to validate the input function extracted by ICA. The sampled bloods were counted using well counter (Packard, U.S.A.). Cross-calibration factor to compensate the difference of counts between PET scanner and well counter was calculated by F-18.

Transaxial images were reconstructed by means of a filtered back-projection algorithm employing a Shepp-Logan filter with cut-off frequency of 0.3 cycles/pixel as 128×128×47 matrices with a size of 2.1×2.1×3.4 mm.

3.2. Preprocessing of $H_2{}^{15}O$ Brain PET Image

Initial 19 frames (< two minute) of PET images were used as an input data for ICA. First, we got static image by summing the dynamic data up to the initial 20 seconds data (4 frames) to find carotid artery region. Since $H_2{}^{15}O$ was injected within 10 seconds, carotid artery could be found

easily in the initial state image where the injected $H_2{}^{15}O$ was not yet distributed in brain tissue or vein better than artery.

On the transverse slice of static images where carotid artery was shown conspicuously, the region regarded as carotid artery was masked to reduce the noise (Figure 2). This mask was also applied to the neighbor 2 slices and those were projected to the dynamic image, thus we got the data set as pixel × pixel × 3 planes × frame matrices. The resulting data were reformatted to frame × pixel matrices for ICA.

4. ICA APPLICATION TO THE DYNAMIC BRAIN $H_2{}^{15}O$ PET IMAGE

4.1 Time-Activity Curve Extraction Using ICA

Frame by pixel data set was used as an input data for the ICA process. All the data points were passed 10 times into the network through the learning rule using a block size of 100 for batch learning. The learning rate was fixed at 0.0005. Log-likelihood was computed continuously to measure the independency of the output of network and determine the optimal repetition time of the training.

TAC of each independent component was obtained from the each column of the basis function **A**, which was computed by inversing the mixing matrix, W and independent component images were also obtained from **u**. We found the rank and sorted independent components in descending order by their contribution extent.

Carotid arterial TAC obtained by ICA method was rescaled to get the true input function. The way to get an scaling factor was similar to that Wu used in their factor analysis approach for FDG and ammonia PET image[12]. The scaling factor was calculated by averaging the counts above a threshold (70% of the maximum) in the corresponding independent component image (carotid artery image).

4.2. Validation of Time-Activity Curves by ICA

For the validation of the carotid arterial TACs by ICA methods, relative error of area under the curve (REAUC) was measured with the arterial sampling data.

Before measuring the AUC, the TACs by ICA were multiplied by the cross calibration factor and shifted as much as the delay from carotid artery to the sampling point. The delay was calculated by comparing the peak time of TACs by ICA with blood sampling.

The equation of REAUC is as follows.

$$REAUC(\%) = \frac{\left| AUC_{sampling} - AUC_{ICA} \right|}{AUC_{sampling}} \times 100 \qquad (6)$$

where $AUC_{sampling}$ is the area under the curve of sampling data and AUC_{ICA} is the area under the curve of carotid arterial TAC by ICA method.

5. RESULTS

In all the cases, carotid artery TACs were extracted successfully by the ICA method. The log-likelihood increased rapidly and reached plateau between 5 and 7 repetition of training as shown in Figure 3. The results were consistent in all the 5 canine studies. Even though we realized the ICA algorithm and reading process of PET image by the low speed computer language, Matlab (Mathworks, Natick, Mass., USA), computation time for whole process was less than 15 seconds on the workstation with 333 MHz CPU and 128 MB memory (DEC AlphaStation 600, Digital Equipment Corp., Maynard, Mass., USA).

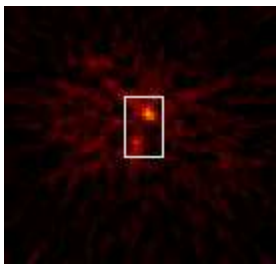

Figure 2. $H_2{}^{15}O$ brain static image and on carotid artery region: Static image was obtained by summing the dynamic image up to initial 20 seconds. Only the carotid arteries are shown prominently comparing to background.

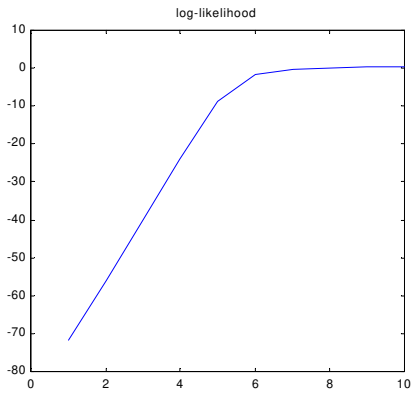

Figure 3. Plot of the log-likelihood of the PDF of the observation during the training as a function of repetition time: it increased rapidly and reached plateau between 5 and 7 repetitions.

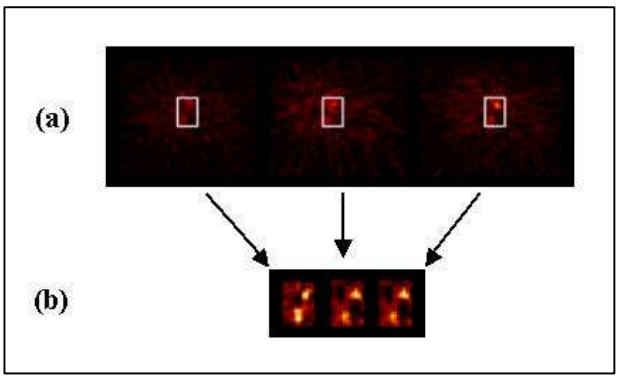

Figure 4. (a) 3 transverse slices of static image (summing 0~20sec) and mask: white square lines are mask used to exclude the unconcerned regions. (b) The resulting independent component image of carotid artery: carotid arteries were well identified in the mask.

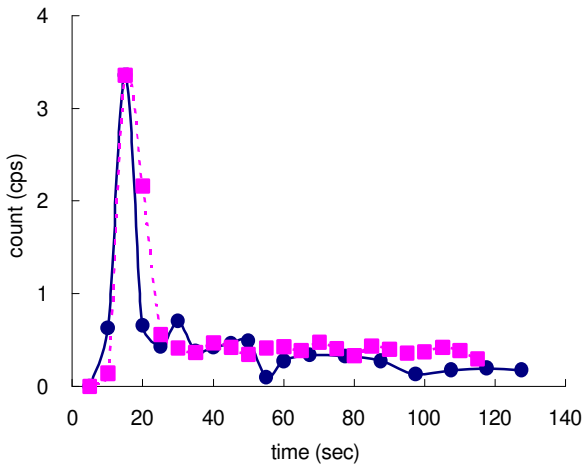

Figure 5. Input functions obtained by ICA method and arterial blood sampling: Rigid line with circle points is the input function from ICA method and dotted line with square points is the one from arterial blood sampling.

Figure 4(a) shows an example of transverse slice of static image on which the ICA performed and Figure 4(b) shows the resulting independent component image of carotid artery. Carotid arteries were well identified in the region of mask.

Input functions by the ICA and blood sampling methods are compared in Figure 5. Solid line with circle point and dashed line with square point are ICA-generated and arterial blood sampled input functions, respectively. Their shapes were very similar except for the tail of the curves and the width around peak region. The widths were smaller in ICA-generated one than blood sampled one. The difference of width around the peak region was increased as $H_2{}^{15}O$ was injected slowly. Thus, the REAUC were varied from 1.6 to 60%.

6. CONCLUSION

The extraction of input function from the images by ICA will be useful for the quantification of the rCBF using dynamic $H_2{}^{15}O$ PET on a clinical situation.

7. REFERENCES

[1] J. Y. Ahn, J. S. Lee, D. S. Lee, J. M. Jeong, J-K. Chung, M. C. Lee, "Multi-plane factor analysis for extracting input functions and tissue curves from O-15 water dynamic myocardial PET", J Nucl Med, Vol. 40(5), p. 77, 1999.

[2] H-M. Wu, et al., J Nucl. Med., 1999;5:36-37

[3] A. S. Houston, "The effect of apex-finding errors on factor images obtained from factor analysis and oblique transformation", Phys Med Biol, Vol. 29, pp. 1109-1116, 1984.

[4] A. S. Houston, W. F. D. Sampson, "A quantitative comparison of some FADS methods in renal dynamic studies using simulated and phantom data", Phys Med Biol, Vol. 42, PP. 199-217, 1997.

[5] M. J. McKeown, S. Makeig, G. G. Brown, T-P. Jung, S. S. Kindermann, A. J. Bell, T. J. Sejnowski, "Analysis of fMRI data by blind separation into independent components", Human Brain Mapping, Vol. 6, pp. 1-31, 1998.

[6] S. Makeig, M. Westerfield, T-P. Jung, J. Covington, J. Townsend, T. J. Sejnowski, E. Courchesne, "Independent components of the late positive event-related potential in a visual spatial attention task" Journal of Neuroscience, Vol. 19, pp. 2665-2680, 1999.

[7] T-W. Lee, Independent component analysis: theory and applications, Boston: Kluwer Academic Publishers., 1998.

[8] J.S. Lee, J.Y. Ahn, D.S. Lee, J.Han, M.J. Jang, J-K, Chung, M.C. Lee, K.S. Park, "Robust Extraction of Input Function from $H_2{}^{15}O$ Dynamic Myocardial Positron Emission Tomography Using Independent Component Analysis"

[9] S. Haykin, Neural network: a comprehensive foundation, UK, London: Prentice-Hall, Inc., pp. 484-544, 1999.

[10] A. J. Bell, T. J. Sejnowski, "An information-maximisation approach to blind separation and blind

deconvolution", Neural Computation, Vol. 7, pp. 1004-1034, 1995.
[11] T-W. Lee, M. Girolami, T.J. Sejnowski, "Independent component analysis using an extended infomax algorithm for mixed sub-gaussian and super-gaussian sources", Neural Computation, Vol. 11, pp. 417-441, 1999.
[12] H-M. Wu, C. K. Hoh, D. B. Buxton, W. G. Kuhle, H. R. Schelbert, Y. Choi, R. A. Hawkins, M. E. Phelps, S-C. Huang, "Quantification of myocardial blood flow using dynamic nitrogen-13-ammonia PET studies and factor analysis of dynamic structures", J Nucl Med, Vol. 36, pp. 2087-2093, 1995.
[13] P. Herrero, J. Markham, D. W. Myears, C. J. Weiheimer, S. R. Bergmann, "Measurement of myocardial blood flow with positron emission tomography: correction for count spillover and partial volume effects", Math Comput Model, Vol. 11, pp. 807-812, 1988.